



Published in final edited form as:

Adv Mater. 2011 November 9; 23(42): 4880–4885. doi:10.1002/adma.201102636.

Viscosity Gradient as a Novel Mechanism for the Centrifugation-Based Separation of Nanoparticles

Dr. Penghe Qiu and

Department of Chemistry and Biochemistry, University of Oklahoma, Stephenson Life Science Research Center, 101 Stephenson Parkway, Norman, OK, 73019, USA

Prof. Chuanbin Mao

Department of Chemistry and Biochemistry, University of Oklahoma, Stephenson Life Science Research Center, 101 Stephenson Parkway, Norman, OK, 73019, USA

Chuanbin Mao: cbmao@ou.edu

Non-uniform size distribution can be observed in the chemical synthesis of many types of nanoparticles. To obtain uniformly distributed nanoparticles, it is necessary to separate them by size. Several size sorting methods have been developed, including size exclusion chromatography,^[1] filtration,^[2,3] electrophoresis,^[4,5] and solvent/antisolvent selective precipitation.^[6] Recently, direct size separation of nanoparticles in the complete liquid phase through centrifugation has been proven to be a more effective method due to its high efficiency, capability of scalable production, and free of nanoparticle aggregation.^[7–9] Both density-based isopycnic centrifugation and velocity-related rate zonal centrifugation have been reported. For small nanoparticles (less than 10 nm), their overall density after solvation falls into the density range of gradient medium, thus isopycnic centrifugation can be used to achieve separation.^[7,9] Larger nanoparticles are generally denser than the liquid medium, so they could only be separated by the difference of sedimentation velocity.^[8–11] Previously, the density gradient has been employed to differentiate the sedimentation velocity of small and large inorganic nanoparticles as well as biological particles.^[8–9,12] In these works, it is widely recognized that variation in the medium density can effectively generate a velocity difference for differently sized nanoparticles and thus achieve separation. However, since the density gradient is created by stacking solutions of a compound of different concentrations, in which not only the density but also the viscosity will be different, the hidden contribution of the viscosity change in the density gradient to separation has not been well realized to date. Here, we used a pure viscosity gradient built from aqueous polyvinylpyrrolidone (PVP) solutions, which have dramatically different viscosities but nearly the same densities among different concentrations, to achieve separation of nanoparticles by size. Our work demonstrates conceptually that the viscosity gradient can be employed as an alternative to the conventional density gradient to achieve highly efficient separation of nanoparticles through rate zonal centrifugation. In methodology, previously only separation of small nanoparticles (less than 25 nm) has been achieved through density gradient, while size nonuniformity also appears in the synthesis of large nanoparticles,^[13–16] thus a size selection process for these nanoparticles is in demand. Here we demonstrate both experimentally and mathematically that the viscosity gradient is more effective in the separation of larger nanoparticles than the density gradient. This is the first report of a size

sorting method for larger nanoparticles (up to 50 nm) with relatively small size difference. We also conducted experiments of separating randomly and widely distributed iron oxide nanoparticle clusters in the PVP viscosity gradient and obtained fairly good purification results based on a single centrifuge run. Extended studies on building a viscosity gradient from PVP of a different molecular weight as well as separation of nanoparticles of different surface capping molecules were also carried out in this work.

PVP (molecular weight, MW, 10 000) is a highly water soluble polymer and can be obtained in a relatively low cost, thus it is chosen here to make the viscosity gradient. The gold nanoparticles (AuNPs) of different sizes are synthesized through a seed-mediated method (see Supporting Information for details). To avoid the aggregation of NPs during centrifugation separation, PVP is used to stabilize the NPs. The PVP-coated AuNPs can maintain the highest stability in the gradient medium, which is highly concentrated PVP, so that the NPs will remain their physical properties after the size separation. As shown in Figure 1A that a small volume of concentrated AuNPs mixture solution, which contained 15, 18, 21, 27, and 31 nm (i.e., five different sizes) NPs, was placed on top of the polymer gradient medium that was built up by 10, 15, 20, 25, and 30 wt% aqueous PVP. After centrifuging at 3400 g for 2.5 h, five fractions of NPs can be seen clearly in the gradient medium. The transmission electron microscopy (TEM) examination (Figures 1B–F) shows that each fraction contains uniformly distributed NPs, with increasing size from top to bottom layers. The statistical study, as shown by the histograms in Figure S1 (Supporting Information) also confirm the high purity of single-sized nanoparticles inside each fraction. In the isopycnic centrifuge, NPs of a particular size and density will stop moving once reaching a liquid layer with a density equal to theirs, and extended centrifuge time will not further shift the relative position of the NPs fractions in the liquid medium. While in the rate zonal centrifuge, as long as there is a centrifugal force, NPs will continue moving downwards even after they have been well separated into several fractions by their sizes. In our approach, it can be seen from photographs taken at 30 min intervals (Figure 1A) that all NPs had been moving downward continuously during the 2.5 h centrifugation time. Therefore, the separation of AuNPs in the PVP viscosity gradient should be through the rate zonal centrifuge, which is by the settling velocity difference among large- and small-sized NPs, rather than the density difference.

The densities of PVP aqueous solutions are only slightly higher than water (1.064 g mL⁻¹ at 30 wt%) and are very close to each other among different concentrations.^[17] The 30 wt% PVP is only about 5% denser than the 10 wt% solution, and there is merely around 1% difference between neighboring layers (Table S1, Supporting Information). However, the viscosity changes dramatically when the polymer concentration varies. The viscosity of 30 wt% PVP is almost 8 times higher than that of 10 wt% PVP solution.^[18] For neighboring layers, the lower layer is 1.6–1.8 times more viscous than the above layer (Table S1, Supporting Information). Hence, one can find that the aqueous PVP concentration gradient will only lead to the formation of viscosity gradient, rather than the density gradient as may happen in many other cases, such as iodixanol, CsCl, and sucrose. Although both density and viscosity increase along with increasing concentration in these examples, they are normally referred as density gradient.

The PVP viscosity gradient contributes in two ways to the successful precise size partition of AuNPs. First, the downward significant increase in viscosity across layer interfaces can effectively impede the smaller NPs from entering the adjacent bottom layer. Larger NPs, although also slowing down, can pass through the interface easily and move toward lower layer to achieve separation. Second, the viscosity gradient narrows the thickness of each NPs fraction so that a good separation resolution can be obtained. For example, when a thin layer of single-sized NPs solution is loaded onto a simple viscosity gradient composed of 15 and

30 wt% PVP (Figure S2 (Supporting Information), time $t = 0$), the NPs can move smoothly in a relatively high velocity into the first low-viscosity PVP layer (15 wt%) under the centrifugal force. Unexpectedly, the NP fraction becomes thicker (Figure S2 (Supporting Information), 12 and 18 min), which is not good for separation of differently sized NPs. Once the frontier NPs in the thick fraction reach the interface of low (15 wt%) and high (30 wt%) viscosity PVP layers, they will experience a sudden decrease in the settling velocity due to the increase in the solution viscosity, while those non-frontier NPs are still moving in the same speed in the 15 wt% PVP layer. Such a velocity different will result in a thinning effect to the NPs fraction at the PVP layer interface (Figure S2 (Supporting Information), 30 and 36 min), which is favored for precise size separation. A viscosity gradient in our work can be described as the vertical downward stacking of many layers of increasing viscosity, which results in the existence of many layer interfaces for thinning each NP fraction. Therefore, the viscosity gradient can precisely separate NPs of different sizes into thin layers with each layer containing NPs of an equal size. In addition to the viscosity gradient, in a swing arm centrifuge rotor, once the larger NPs are slightly separated from the smaller ones, they will go through a higher centrifugal g force, due to the increase of actual radius of rotation, which will raise the settling velocity of larger NPs and further favors partition.

Although PVP (10 000) can be dissolved as high as 60 wt% in water, the best concentration range that is suitable to build the viscosity gradient is 10–40 wt%. When PVP is lower than 10 wt%, the viscosity of its solution is only slightly higher than that of water. Such low viscosity is practically difficult to create an interface between PVP solutions of different concentrations. For example, when a 3 wt% PVP solution is loaded onto an 8 wt% one, instead of forming a new layer on the top of the underneath solution, which is what happens when loading PVP solutions used in Figure 1A, the former enters directly and deeply into the latter, leaving no interface between the two solutions. And same thing will happen when nanoparticles solution is placed on top of the low-concentration PVP solutions. However, the interfaces and a thin layer of nanoparticles solution on the topmost are both indispensable for the good size separation of nanoparticles. On the other hand, in solutions containing more than 40 wt% PVP, their viscosities are so high that regular handling of the solutions, like transferring from one container to another, will be very difficult with common laboratory tools. More importantly, when nanoparticles are moving down in the multilayer PVP viscosity gradient under centrifugal force, they will experience extremely high resistance force to enter into a layer with high viscosity, which is caused by the excessive concentration of PVP in that layer. As a result, both large and small nanoparticles will be blocked at the interface, achieving no further size separation. For NPs of a specific size range, the selection of PVP concentrations to build the viscosity gradient should follow the general rule that the bottom PVP layer, which has the highest PVP concentration, should be viscous enough to effectively impede the travel of the largest NPs in the sample, while the topmost PVP layer, which has the lowest PVP concentration, should not be too viscous for the entrance of the smallest NPs in the sample (see Figure S3 (Supporting Information) for detailed discussion).

The density gradient has been demonstrated as a very effective method for separation of small NPs through isopycnic centrifuge, in which the density difference among gradients mainly contributes to the separation. For large NPs, for instance 30 nm or larger AuNPs, their overall density will be much higher than that of the liquid. Separation of NPs can only be realized through a rate zonal centrifuge. In such circumstances, the density gradient may not be sufficient to retard particle sedimentation or regulate the NPs fraction thickness. The settling velocity of nanoparticles in a medium can be described by Stokes' law in the Equation S1 (Supporting Information).^[19] Based on this equation, we did some simple calculation and made a comparison of the effectiveness of the density gradient and the viscosity gradient in the separation of large NPs. We assumed that the viscosity of liquids in

a density gradient is constant and vice versa. According to the work by Falabella et al.^[20] it is very reasonable to assume large AuNPs (more than 10 nm) having density of 5 g cm^{-3} or even higher. Considering a nanoparticle of 5 g cm^{-3} density, when it settles from 1 g mL^{-1} to 2 g mL^{-1} medium, which is about the highest density a typical liquid medium can reach, the settling velocity will only be reduced by 25% (refer to Equation S1 (Supporting Information) for detailed calculation and discussion). The PVP-based viscosity gradient, however, achieves separation of NPs uniquely by viscosity, regardless the density of medium. As mentioned above that the viscosity of 30 wt% PVP will increase up to nearly 8 times that of 10 wt% PVP, the settling velocity of NPs, as calculated by Stokes' law,^[19] in the former will be 1/8 of that in the latter. And this is true for NPs of any size. It has been discussed in the above paragraphs, as well as in literature, that the size separation of NPs is primarily because of the sharp decrease of the settling velocity of the NPs at the gradient interface. Therefore, the viscosity gradient is more likely capable of partitioning larger NPs. As a demonstration, uniform 31, 44, and 50 nm AuNPs were mixed up and centrifuged in 20, 25, 30, 35, and 40 wt% PVP viscosity gradient, three fractions corresponding to each size of NPs can be obtained after centrifuge (Figure 2A; see also Figure S4 (Supporting Information) for TEM images). It should be noted that in previous reports, all approaches on size separation had focused on NPs below 25 nm, so this is the first attempt to separate large NPs.

The viscosity of polymer is dependent on its MW. Under the same concentration, polymer of higher MW will have a higher viscosity. In other words, to obtain the same viscosity, less concentrated high MW polymer can be used; this provides more flexibility to minimize the cost of separation through viscosity gradient. Here, besides using PVP 10 000, we also tried to employ PVP 40 000 for separation of AuNPs (see Table S2 (Supporting Information) for viscosity and density profile). For five sized NPs (same as those in Figure 1), 5.8, 8.7, 11.8, 14.8, and 18.7 wt% PVP 40 000, whose viscosities are equivalent to 10, 15, 20, 25, and 30 wt% PVP 10 000, were used to build the viscosity gradient. The centrifugation was carried out under the same conditions, and finally five NPs fractions that are similar to Figure 1 were obtained (Figure 2B and Figure S5, Supporting Information). More importantly, no destabilization of the NPs was found under higher MW polymer solution. Similarly, when everything else was remained identical to Figure 2A, but the polymer concentration changed to 11.8, 14.8, 18.7, 22.8, and 27.0 wt% PVP 40 000, three fractions of larger AuNPs can be observed (Figure 2C and Figure S6, Supporting Information). It is expected that with even higher PVP MW, the concentration needed to build viscosity gradient could be further reduced.

Up to this point, all of our demonstrations of nanoparticles size separation are based on the PVP-covered AuNPs. However, hydrophilic nanoparticles have been synthesized with many other surface capping molecules, such as surfactants,^[13–14] thiol-containing charged small molecules,^[21] and other polymers.^[22–24] Most of the non-PVP coated nanoparticles will be destabilized in solutions with a high PVP concentration and thus the polymer-based viscosity gradient is not suitable for direct size separation of these nanoparticles. However, we found that in solutions containing both high concentration of PVP and a proper amount of the surface capping molecules, e.g., cetyl trimethyl ammonium bromide (CTAB), the corresponding nanoparticles (CTAB-capped) can be dispersed without any destabilization or aggregation. By incorporating the surface capping molecules into each layer of the PVP viscosity gradient, the size separation of non-PVP-stabilized nanoparticles can be achieved. As shown in Figure 3A-1, the viscosity gradient was built by stacking 15, 30, and 40 wt% PVP (10 000) in a 1.5 mL eppendorf tube and each PVP layer contained 0.1 M CTAB. A thin layer of concentrated CTAB-stabilized AuNPs of two different sizes (12 nm and 24 nm) was loaded on the topmost of the viscosity gradient. Two distinct nanoparticles fractions could be observed after centrifuge at 9660 g for 40 min (Figure 3A-2). The two

nanoparticles fractions were extracted, diluted, centrifuged, and redispersed into water. The resulting nanoparticles solutions were then compared with the two as-prepared pure AuNPs solutions shown in Figure 3B. Their optical spectra showed no remarkable difference (Figure 3C), indicating that no destabilization or aggregation of CTAB-covered AuNPs took place after separation in the PVP viscosity gradient. TEM examination (Figure 3D,E) also confirmed the individual dispersion and uniform size distribution of AuNPs in the two fractions shown in Figure 3A-2. As a contrast, when the same CTAB-covered AuNPs were loaded onto the same PVP viscosity gradient but without 0.1 M predissolved CTAB, serious aggregation that was indicated by the nanoparticles' color change (Figure 3A-3)^[25-26] happened once the nanoparticles entered into the PVP layer under centrifugal force. When the aggregated AuNPs were collected through a similar extraction, dilution, and centrifugation process, they were not able to redisperse into water, indicating that the aggregation of nanoparticles in the PVP viscosity gradient without predissolved CTAB is non-reversible.

In our recent work, we reported that iron oxide nanoparticle clusters (NPCs) can be formed by selective phase evaporation in a CTAB-based oil-in-water emulsion system.^[16] The as-synthesized NPCs were not uniform in size. Although NPCs smaller than 30 nm can be separated through differential centrifuge, the rest of the nanoparticles were still widely distributed between 30–150 nm (Figure 4A and Figure S7, Supporting Information). Since the destabilization issue of non-PVP stabilized nanoparticles has been solved, here we made our attempt to separate CTAB covered iron oxide NPCs in the PVP viscosity gradient. The solutions of PVP with a molecular weight of 40 000, which are colorless and thus make it easier to discern the movement of yellowish NPCs, were employed to build the viscosity gradient. From top to bottom (Figure 4B, left), the viscosities were equivalent to those in 10, 15, 20, 25, and 30 wt% PVP (with a molecular weight of 10 000) solutions, respectively. In all of our previous demonstrations, model samples that contain only three or five differently sized nanoparticles were used and the separation treatment resulted in several distinct nanoparticle fractions, each corresponding to nanoparticles of a single size. However, the iron oxide NPCs are randomly sized and their size distribution is not discrete. After centrifugation for 2.5 h, we observed no apparent nanoparticle fractions, but continuous distribution of NPCs through different layers of PVP viscosity gradient (Figure 4B, the variation of the darkness of the yellow color in the pictures might be caused by the concentration difference of NPCs). A small volume of samples (300 μ L) was taken out by a needle at four random sites as indicated by arrows in Figure 4B. The TEM examinations (Figure 4C–F) revealed that the NPCs had been separated by size in the PVP viscosity gradient. The smaller NPCs were left in the top layers, while larger particles moved down to the bottom layers. From low magnification TEM images as well as the statistical study (Figure S8,S9, Supporting Information), it can be seen that the size distribution of NPCs had been significantly narrowed down, compared to that of the as-synthesized nanoparticles. Given that there has been no example in the literature about the separation of randomly distributed nanoparticles with such a large size variation (30–150 nm), the PVP viscosity gradient can be a very useful and unique tool to purify this type of nanoparticles. Although the size of iron oxide NPCs in each fraction is not completely uniform, we are optimistic that through another round of separation, in a properly built viscosity gradient, the distribution will be further improved.^[8]

As a summary, a novel method for precise size sorting of NPs through the PVP-based viscosity gradient is developed. PVP-stabilized AuNPs of small size difference can be separated into different fractions with an excellent resolution. The contribution of the viscosity gradient to the successful size separation of NPs was discussed. The viscosity gradient has been proved to be more powerful than density gradient in separating larger NPs. PVP solutions of different polymer molecular weights, but having equivalent viscosity, were

used to obtain similar separation results, demonstrating the flexibility of the novel method. Finally, we demonstrated that the PVP viscosity gradient can be used to separate AuNPs and iron oxide NPCs with a different surface chemistry by predissolving a proper concentration of the corresponding surface capping molecules into the viscosity gradient. The weight of 18 nm AuNPs is only 1.73 times that of 15 nm particles, and 31 nm particles are merely 1.51 times as heavy as 27 nm particles. The precise separation of NPs of tiny size difference makes the viscosity gradient very promising in purification of NPs dimers and trimers from individual ones without using high ionic-strength medium, which will destabilize NPs in most cases.^[8] The settling velocity difference is only dependent on the size or shape and density of the NPs and is not related to their other physical or chemical properties.^[19] Thus, although only nanoparticles of Au and Fe₃O₄ were used in the experimental demonstrations, the PVP viscosity gradient may be extended to separate NPs of other materials. Finally, PVP and CTAB are the two major capping reagents that have played critical roles in the shape-defined synthesis of many types of noble metallic NPs, however, nonuniform size distribution can be found in a number of these NPs,^[13–14,27–33] the viscosity gradient developed here should be readily applied to purify them.

Supplementary Material

Refer to Web version on PubMed Central for supplementary material.

Acknowledgments

The authors thank the National Science Foundation (DMR-0847758, CBET-0854414, CBET-0854465), National Institutes of Health (R21EB009909-01A1, R03AR056848-01, R01HL092526-01A2), and Oklahoma Center for the Advancement of Science and Technology (HR11-006) for the financial support.

References

1. Novak JP, Nickerson C, Franzen S, Feldheim DL. *Anal Chem.* 2001; 73:5758. [PubMed: 11774918]
2. Akthakul A, Hochbaum AI, Stellacci F, Mayes AM. *Adv Mater.* 2005; 17:532.
3. Sweeney SF, Woehrlé GH, Hutchison JE. *J Am Chem Soc.* 2006; 128:3190. [PubMed: 16522099]
4. Hanauer M, Pierrat S, Zins I, Lotz A, Sonnichsen C. *Nano Lett.* 2007; 7:2881. [PubMed: 17718532]
5. Xu XY, Caswell KK, Tucker E, Kabisatpathy S, Brodhacker KL, Scrivens WA. *J Chromatogr A.* 2007; 1167:35. [PubMed: 17804004]
6. McLeod MC, Anand M, Kitchens CL, Roberts CB. *Nano Lett.* 2005; 5:461. [PubMed: 15755095]
7. Bai L, Ma XJ, Liu JF, Sun XM, Zhao DY, Evans DG. *J Am Chem Soc.* 2010; 132:2333. [PubMed: 20121127]
8. Chen G, Wang Y, Tan LH, Yang MX, Tan LS, Chen Y, Chen HY. *J Am Chem Soc.* 2009; 131:4218. [PubMed: 19275162]
9. Sun XM, Tabakman SM, Seo WS, Zhang L, Zhang GY, Sherlock S, Bai L, Dai HJ. *Angew Chem Int Ed.* 2009; 48:939.
10. Wu T, Wang XJ, Li GP, Chen T, Yang MX, Zhang Z, Chen HY. *Nano Lett.* 2008; 8:2643. [PubMed: 18672944]
11. Chen HY, Wang Y, Chen G, Yang MX, Silber G, Xing SX, Tan LH, Wang F, Feng YH, Liu XG, Li SZ. *Nat Commun.* 2010; 1:1. [PubMed: 20975674]
12. Anderson, NG. The development of zonal centrifuges and ancillary systems for tissue fractionation and analysis. U.S. Dept. of Health, Education, and Welfare, Public Health Service, National Cancer Institute; United States: 1966.
13. Millstone JE, Park S, Shuford KL, Qin LD, Schatz GC, Mirkin CA. *J Am Chem Soc.* 2005; 127:5312. [PubMed: 15826156]
14. Busbee BD, Obare SO, Murphy CJ. *Adv Mater.* 2003; 15:414.

15. Jin RC, Cao YC, Hao EC, Metraux GS, Schatz GC, Mirkin CA. *Nature*. 2003; 425:487. [PubMed: 14523440]
16. Qiu PH, Jensen C, Charity N, Towner R, Mao CB. *J Am Chem Soc*. 2010; 132:17724. [PubMed: 21117657]
17. Sadeghi R, Zafarani-Moattar MT. *J Chem Thermodyn*. 2004; 36:665.
18. Davidson, RL.; Sittig, M. *Water-Soluble Resins*. Reinhold Publishing Corporation; New York: 1962.
19. Lamb, H. *Hydrodynamics*. Cambridge University Press; Cambridge, UK: 1975.
20. Falabella JB, Cho TJ, Ripple DC, Hackley VA, Tarlov MJ. *Langmuir*. 2010; 26:12740. [PubMed: 20604538]
21. Sperling RA, Parak WJ. *Phil Trans R Soc A*. 2010; 368:1333. [PubMed: 20156828]
22. Ge J, Hu Y, Biasini M, Beyermann WP, Yin Y. *Angew Chem Int Ed*. 2007; 46:4342.
23. Mayya KS, Schoeler B, Caruso F. *Adv Funct Mater*. 2003; 13:183.
24. Gittins DI, Caruso F. *J Phys Chem B*. 2001; 105:6846.
25. Lee JS, Ulmann PA, Han MS, Mirkin CA. *Nano Lett*. 2008; 8:529. [PubMed: 18205426]
26. Kim JY, Lee JS. *Nano Lett*. 2009; 9:4564. [PubMed: 19928782]
27. Nikoobakht B, El-Sayed MA. *Chem Mater*. 2003; 15:1957.
28. Lim B, Xiong Y, Xia Y. *Angew Chem*. 2007; 119:9439.
29. Washio I, Xiong Y, Yin Y, Xia Y. *Adv Mater*. 2006; 18:1745.
30. Camargo PHC, Xiong Y, Ji L, Zuo JM, Xia Y. *J Am Chem Soc*. 2007; 129:15452. [PubMed: 18027954]
31. Xiong Y, Cai H, Wiley BJ, Wang J, Kim MJ, Xia Y. *J Am Chem Soc*. 2007; 129:3665. [PubMed: 17335211]
32. Ha TH, Koo HJ, Chung BH. *J Phys Chem C*. 2007; 111:1123.
33. Zhang H, Xia XH, Li WY, Zeng J, Dai YQ, Yang DR, Xia YN. *Angew Chem Int Ed*. 2010; 49:5296.

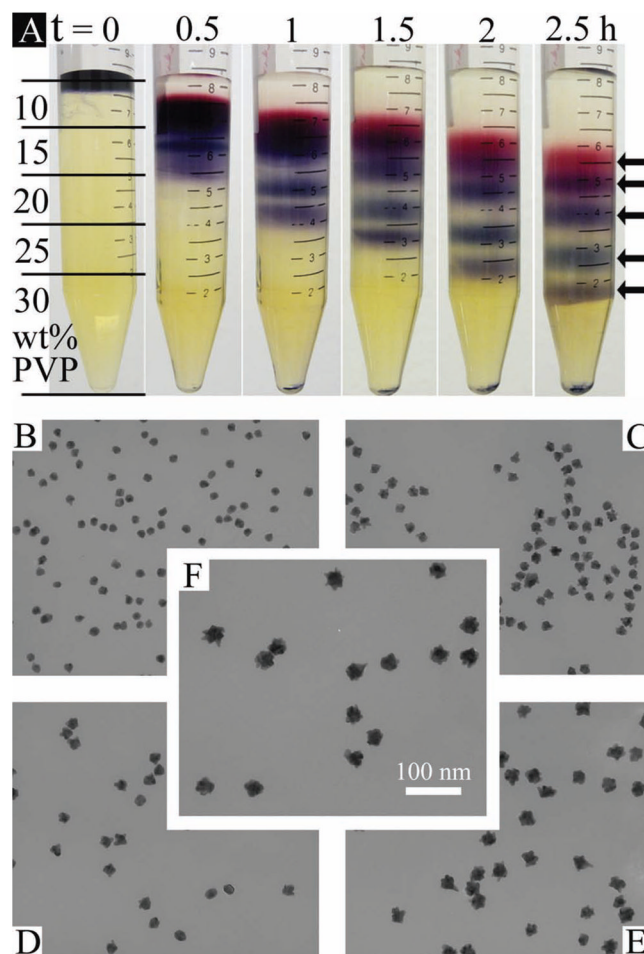


Figure 1. Separation of 15, 18, 21, 27, and 31 nm five differently sized AuNPs in a PVP 10 000 viscosity gradient. A) Photographs taken at 0.5 h intervals. Gradient thickness is indicated by black lines on the leftmost tube. Five NPs fractions, indicated by arrows, can be seen clearly after 2.5 h of centrifugation. B–F) TEM images, corresponding to fractions from top to bottom, show NPs size in each fraction. Scale bar in (F) is applicable to all images.

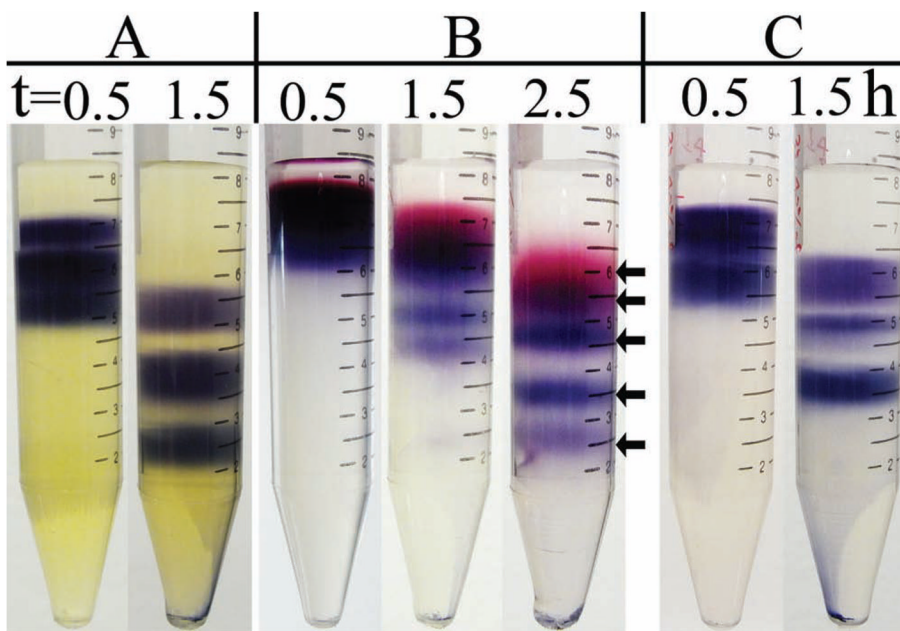


Figure 2.

A) Separation of 31, 44, and 50 nm large AuNPs in 20, 25, 30, 35, and 40 wt% PVP 10 000 viscosity gradient. B) Separation of five differently sized AuNPs in 5.8, 8.7, 11.8, 14.8, and 18.7 wt% PVP 40 000 viscosity gradient. Five NPs fractions are indicated by arrows. NPs sizes and viscosities of each gradient are the same as in Figure 1. C) Separation of three differently sized AuNPs in 11.8, 14.8, 18.7, 22.8, and 27.0 wt% PVP 40 000 viscosity gradient. NPs sizes and viscosities of each gradient are the same as in Figure 2A. In all images, gradients are built identical to the structure in the leftmost part of Figure 1A.

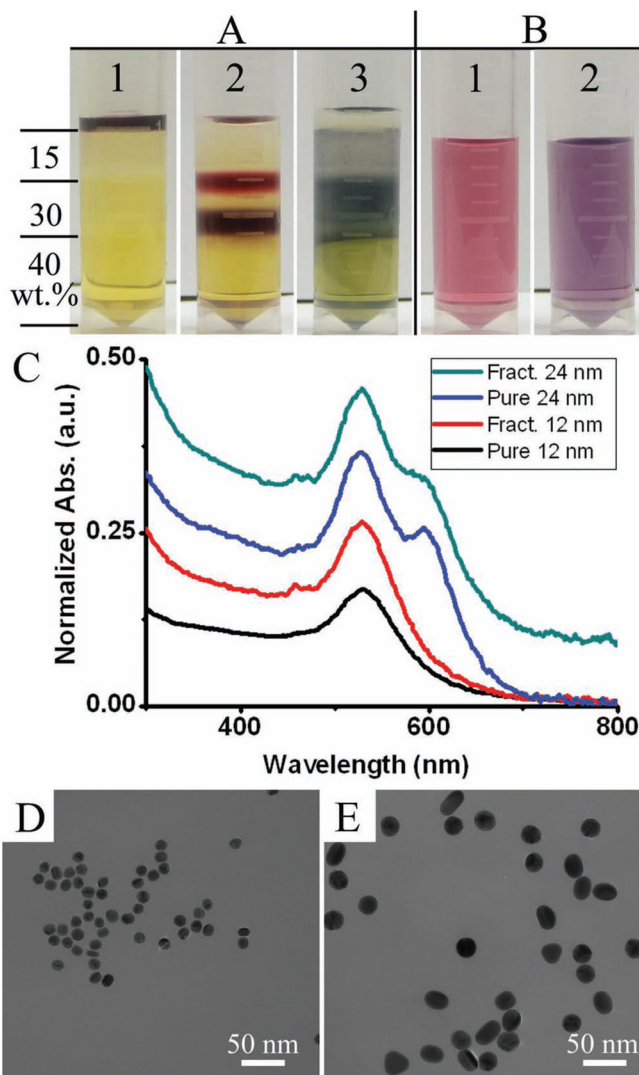


Figure 3. Separation of 12 and 24 nm CTAB covered AuNPs in the PVP viscosity gradient. A) Photographs showing 1) structure of the viscosity gradient, 2) two AuNPs fractions, corresponding to 12 nm (top fraction) and 24 nm (bottom fraction) NPs, formed after 40 min centrifuge at 9660 g in the PVP viscosity gradient that has 0.1 M predissolved CTAB, and 3) aggregation of CTAB covered AuNPs in PVP viscosity gradient that has no predissolved CTAB, taken after 10 min centrifuge at 9660 g. B) Photographs showing the colors of the as-prepared pure CTAB covered AuNPs: 1) 12 nm and 2) 24 nm. C) Optical absorption spectra of the as-prepared pure CTAB-AuNPs in Figure 3B and the viscosity gradient separated AuNPs in the fractions in Figure 3A-2. D,E) TEM images of the two AuNPs fractions in Figure 3A-2, showing the size uniformity and free of aggregation after separation in the PVP viscosity gradient.

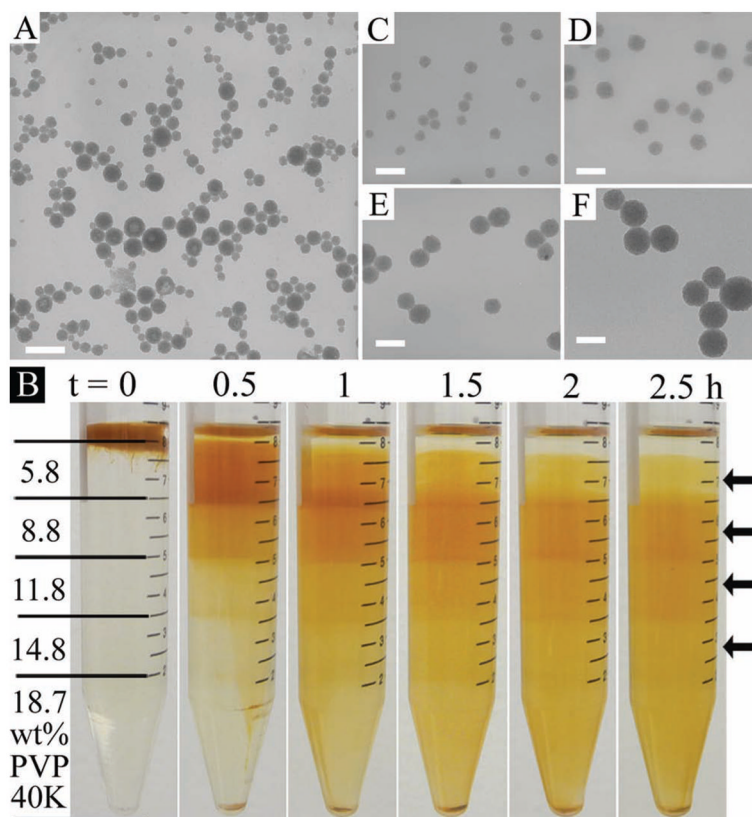


Figure 4. Separation of iron oxide nanoparticle clusters (NPCs) which are randomly distributed between 30 to 150 nm. A) TEM image of the as-synthesized NPCs. B) Photographs taken at 30 min intervals during the centrifugation. The structure of the viscosity gradient is marked on the leftmost tube. Each PVP solution has 0.1 M CTAB dissolved to prevent aggregation of nanoparticles. C–F) TEM images of NPCs corresponding to the sites (top to bottom) indicated by arrows in (B). Scale bars: 200 nm in (A) and 100 nm in (C–F).